INTERNATIONAL JOURNAL FOR NUMERICAL METHODS IN FLUIDS
Int. J. Numer. Meth. Fluids 2006; **51**:635–657
Published online 20 December 2005 in Wiley InterScience (www.interscience.wiley.com). DOI: 10.1002/fld.1144

A priori tests on numerical errors in large eddy simulation using finite differences and explicit filtering

Tellervo Brandt*,†

Laboratory of Aerodynamics, Helsinki University of Technology, P.O. Box 4400, FIN-02015 TKK, Finland

SUMMARY

When low-order finite-difference methods are applied in large eddy simulation (LES), the magnitude of the numerical error may be larger than that of the subgrid-scale (SGS) term. In this paper, the effect of explicit filtering on the numerical error related to the spatial discretization of the convection term and the exact SGS term is studied *a priori* in the turbulent fully developed channel flow. As the filter width is increased the grid resolution is kept constant. Also filtering in the inhomogeneous wall-normal direction is discussed. The main conclusions are related to two approaches to explicit filtering. In the traditional approach, the whole velocity field is filtered explicitly while in the alternative approach, only the non-linear convection term of the Navier–Stokes equations is filtered explicitly. Based on the results presented in the paper it seems that the first approach leads to an unphysical situation. However, the later approach works in the desired way, and the numerical error becomes clearly smaller than the SGS term. The main difference between the two approaches seems to be the interpretation of the resolved non-linear term in the filtered Navier–Stokes equations. Copyright © 2005 John Wiley & Sons, Ltd.

KEY WORDS: LES; numerical error; explicit filtering; *a priori* testing

1. INTRODUCTION

The starting point in direct numerical simulation of turbulence (DNS) are the Navier–Stokes equations. Although analytical solutions of these equations are known only for some laminar cases, at the moment it is widely believed that the Navier–Stokes equations describe also turbulent flows. In DNS, all the turbulent motion is solved numerically from the Navier–Stokes equations and no models are applied. This approach requires a huge amount of computer capacity, and thus, it is mainly a research tool [1].

*Correspondence to: T. Brandt, Laboratory of Aerodynamics, Helsinki University of Technology, P.O. Box 4400, FIN-02015 TKK, Finland.
†E-mail: Tellervo.Brandt@tkk.fi

Contract/grant sponsor: Finnish National Graduate School in Computational Fluid Dynamics
Contract/grant sponsor: Finnish Cultural Foundation

Received 27 February 2005
Revised 30 September 2005
Accepted 18 October 2005

In large eddy simulation (LES), the Navier–Stokes equations are filtered using a low-pass filter. The scales of motion are divided into two parts: the resolved and sub-filter-scale motions. Only the resolved scales are simulated accurately and the effect of the sub-filter scales on the larger scales is modelled. Usually, in finite-difference calculations, the grid itself is interpreted as an implicit filter and no explicit filtering is applied. Thus, the two scales are named as resolved and subgrid scales (SGS).

When one performs simulations in complex geometries, spectral discretization methods are not a suitable choice, and finite-difference-type or finite-element schemes are applied. However, with commonly applied low-order finite-difference schemes numerical error, mainly truncation error, becomes a problem. This error may dominate the SGS term and even using an advanced SGS model will not improve the situation [2].

When finite-difference-type methods are applied, the truncation error has the strongest effect on the smallest resolved scales, which are badly described by the grid. If the grid resolution is increased, the numerical error related to the resolved scales of the coarser grid diminishes, but at the same time there will be new small scales present, and these scales are again contaminated by numerical error. In addition, the effect of the SGS model will diminish with increased resolution. Thus, even after grid refinement, the dominance of the SGS term over the numerical error is not necessarily clear. Applying high-order methods would improve the situation, but as the truncation error is reduced aliasing error may become a problem [3].

The dominance of the numerical error over the SGS term has been studied *a priori* using DNS data by several groups [2, 4–6], and explicit filtering has been suggested as a cure for the problem. As the small scales are removed and considered as SGS, the magnitude of the numerical error related to the resolved scales reduces. At the same time, the responsibility for these scales should be shifted to the SGS model, and thus, the effect of the model should increase. Some of the studies have been performed applying finite-difference schemes [4, 5], and in some studies the spectral methods with modified wave numbers have been applied [6]. For the second-order central-difference scheme, an explicit filter with the width of four grid spacings has been recommended [6].

Also actual LES applying explicit filtering have been presented [7–9]. In the simulations, there have been two approaches to explicit filtering. The traditional choice is to filter the whole velocity field as done in Reference [7]. The other option is to filter only the non-linear convection term of the Navier–Stokes equations as suggested in Reference [10]. This approach has been applied in actual LES in References [8, 9].

In the simulations applying explicit filtering, the benefit is unclear if one considers the increased computing effort [7]. However, when compared to traditional approaches improved results have been obtained [8]. When explicit filtering is applied, the roles of the SGS model and the numerical error are clear and if the behaviour of the SGS model is considered, good or bad results can be explained with increased certainty.

In this paper, both mentioned approaches to explicit filtering are studied *a priori*. The fully developed turbulent channel flow between two parallel walls is applied as a test case, and we concentrate on the second-order finite-difference scheme that is widely used in practical simulations. The aim is to gain more information on how explicit filtering could be used in actual LES where the grid resolution is limited by computer capacity. Here, the grid resolution is not increased with increasing filter width, and thus, increasing the filter width leads to lower nominal resolution. In this paper, we only consider the magnitudes of the exact SGS term and the numerical error related to the finite-difference approximation of convection term of

the Navier–Stokes equations. Thus, modelling error or numerical error due to time integration are not discussed.

Previously, in the *a priori* tests involving inhomogeneous directions, filtering has been performed only in homogeneous directions. In this paper, we discuss also *a priori* tests where filtering is applied in the wall-normal direction. The applied filter is an approximation to the spectral cut-off filter and the related commutation error is of fourth order [11].

In Section 2, the numerical schemes applied in the DNS simulations are discussed. In Section 3, we discuss the chosen test cases, and in Section 4, the results of *a priori* tests are presented and discussed. In Section 4, the results for the two mentioned approaches to explicit filtering are first studied using two-dimensional filtering. The difference between the approaches is discussed, and finally the tests are repeated applying three-dimensional filters.

2. NUMERICAL METHODS

The equations describing the flow of an incompressible Newtonian fluid—i.e. the Navier–Stokes equations may be written in the non-dimensional form as

$$\frac{\partial u_j}{\partial x_j} = 0 \tag{1}$$

$$\frac{\partial u_i}{\partial t} = -\frac{\partial p}{\partial x_i} + \frac{\partial}{\partial x_j}\left(-u_i u_j + \frac{1}{Re_\tau}\left(\frac{\partial u_i}{\partial x_j} + \frac{\partial u_j}{\partial x_i}\right)\right) \tag{2}$$

where $u_i (i = 1, 2, 3)$ is the non-dimensional velocity component in the ith coordinate direction, p is the non-dimensional pressure and Re_τ is the Reynolds number. Hereafter, u_i refers to velocity scaled by the friction velocity, u_τ, x_i to coordinate scaled by the channel half-height, δ, t to time scaled by u_τ/δ and p to pressure scaled by ρu_τ^2. The Reynolds number is here defined as

$$Re_\tau = \frac{u_\tau \delta}{v} \tag{3}$$

In the channel flow, there are two homogeneous directions: the streamwise and the spanwise. Periodic boundary conditions were applied in these directions, and no-slip conditions were forced on the top and bottom walls.

In the chosen coordinate system, x-axis points in the streamwise direction, y-axis in the spanwise and z-axis in the wall-normal direction. Correspondingly, the streamwise velocity component is referred to as u, the spanwise as v and the wall normal as w.

The spatial derivatives are evaluated applying the second-order central-difference scheme on a staggered grid from Reference [12]. In the staggered grid system, pressure points are located at the centre of a computational cell and the velocity points on the boundaries. The streamwise velocity point is on the boundary normal to the streamwise component, etc. The advantage of using the staggered grid is that we have a strong coupling between velocity and pressure, and thus, oscillating pressure modes are avoided. In addition, the second-order central-difference scheme conserves kinetic energy only on the staggered grid system [13].

For time integration, a low-storage, third-order, three-stage, explicit Runge–Kutta method from Reference [14] was applied to the convection and diffusion terms of Equation (2). This

Table I. The coefficients of the applied Runge–Kutta method on the three intermediate time steps.

	1st step	2nd step	3rd step
c_1	8/15	5/12	3/4
c_2	0	−17/60	−5/12

method involves in all three intermediate time steps inside one physical time step, and one intermediate step may be written as

$$u_i^{*,n+1} = u_i^n + \Delta t^n (c_1^n \Delta u_i^n + c_2^n \Delta u_i^{n-1}) \tag{4}$$

where the superindices refer to (intermediate) time levels, Δt is the time step, c_1 and c_2 are the coefficients that vary on each intermediate time step (Table I) and Δu_i is the discrete form of the convection and diffusion terms of Equations (2). u_i^* is the so-called predicted velocity field that does not necessarily satisfy the continuity equation (Equation (1)). The fluctuating pressure is solved on each intermediate time step from the Poisson equation

$$\frac{\partial^2 p^{n+1}}{\partial x_i x_i} = \frac{\partial u_i^{*,n+1}}{\partial x_i} \tag{5}$$

where periodic boundary conditions are applied, and the predicted velocity field is corrected by the fluctuating pressure gradient as

$$u_i^{n+1} = u_i^{*,n+1} + \frac{\partial p^{n+1}}{\partial x_i} \tag{6}$$

In the fully developed channel flow, there is mean-pressure gradient only in the streamwise direction, and this pressure gradient drives the flow. When the equations are scaled by the friction velocity, the non-dimensional mean-pressure gradient equals 2 (see Reference [15]), and in the present simulations the mean-pressure gradient was fixed to this value and the mean velocity was let to vary. The time-integration method allows the Courant number (CFL) of 1.7 [14], but here value 1 was applied. To keep the Courant number fixed, the physical time step was allowed to vary.

3. TEST CASES AND DNS RESULTS

In this section, we discuss the DNS data from the fully developed channel flow applied in the *a priori* tests. The aim is to verify that the DNS is sufficiently well resolved for these tests. The dimensions of the channel and the chosen grid resolution in DNS for the $Re_\tau = 180$ case are given in Table II and for the $Re_\tau = 395$ case in Table III.

The mean-velocity profile and the root-mean squares (RMS) of the fluctuating velocity components ($u_{\mathrm{RMS}} = \sqrt{\langle u'u' \rangle}$) scaled by the friction velocity from the simulation at $Re_\tau = 180$ are given in Figures 1 and 2, respectively, and the turbulent, viscous and total stresses in Figure 3. The reference data are from the simulations of Moser *et al.* [16] (MKM).

Table II. Dimensions of the channel and grid resolution in the DNS at $Re_\tau = 180$.

	Streamwise	Spanwise	Wall-normal
Length/channel half-height	8.0	4.0	2.0
Length in wall units	1440	720	360
Number of grid points	120	150	100
Size of grid cells in wall units	12	5	6 (max) 0.4 (min)

Wall units: $x^+ = Re_\tau x$, where x is scaled by the channel half-height.

Table III. Dimensions of the channel and grid resolution in the DNS at $Re_\tau = 395$.

	Streamwise	Spanwise	Wall-normal
Length/channel half-height	6.0	3.2	2.0
Length in wall units	2370	1264	790
Number of grid points	160	160	120
Size of grid cells in wall units	15	8	15 (max) 0.7 (min)

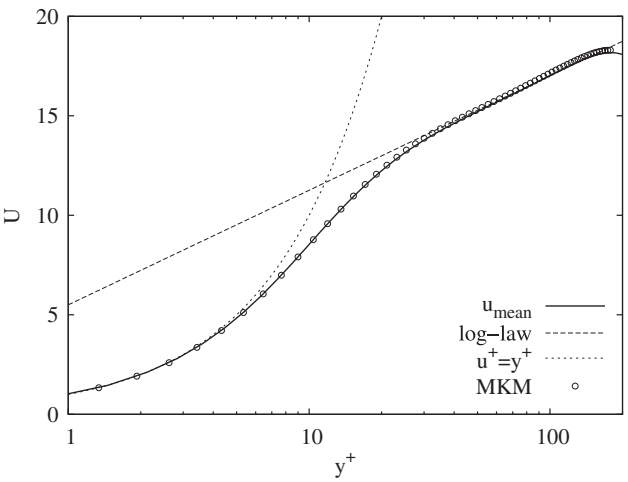

Figure 1. Mean velocity profile. $Re_\tau = 180$.

One-dimensional streamwise and spanwise energy spectra are plotted in Figure 4. The streamwise one-dimensional spectrum is plotted in the middle of the channel and the spanwise in the near-wall region. In addition, spectra from $y^+ \approx 36$ is included. They are required later in this paper. We see that the spectra drop off several orders of magnitude, and thus, the grid resolution seems adequate.

In Figure 5, the mean-velocity profile is plotted from the $Re_\tau = 395$ case. The mean velocity is underpredicted when compared to the reference data. The RMS-velocities are given in Figure 6. Here, the streamwise Reynolds stress is underpredicted. The total, viscous and

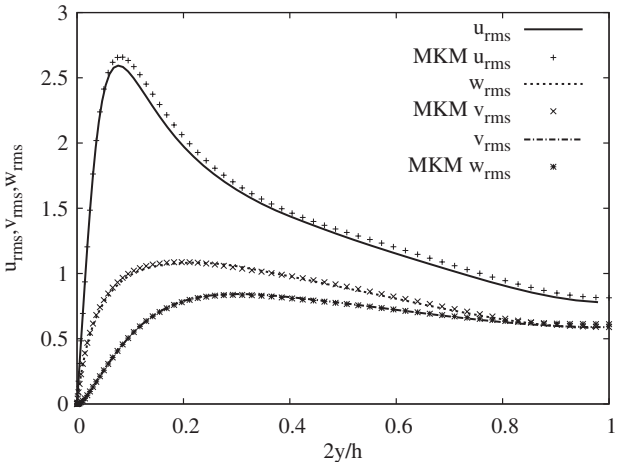

Figure 2. The RMS-velocity components. $Re_\tau = 180$.

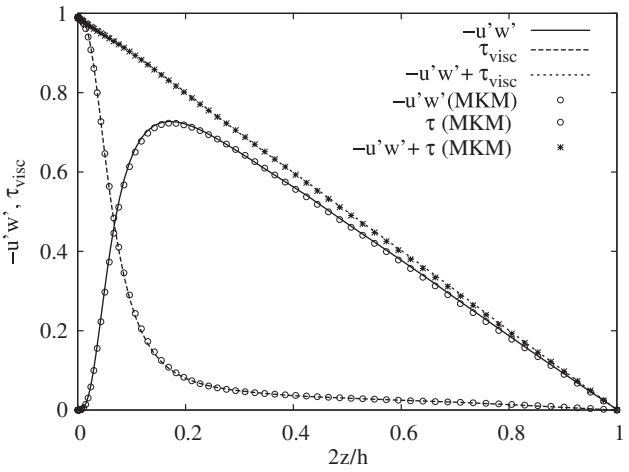

Figure 3. Turbulent, viscous and total stresses. $Re_\tau = 180$.

turbulent stresses are depicted in Figure 7. The streamwise one-dimensional energy spectrum is plotted in Figure 8 in the middle of the channel, and the spanwise in the near-wall region ($z^+ \approx 5$). The spectra drop off, but in the spanwise direction the resolution could be further improved. At this larger Reynolds number, the simulation is thus not as well resolved as at the lower Reynolds number. However, the *a priori* tests were repeated using grids with both lower and larger resolutions, and the conclusions of the tests were not sensitive to the grid refinement. The resolution of the DNS was thus considered adequate for these *a priori* tests.

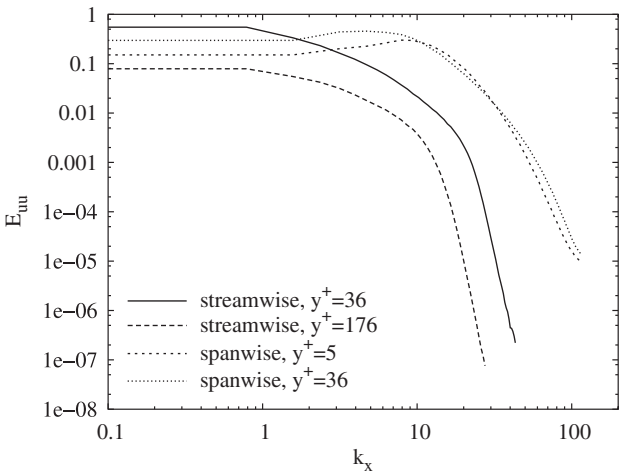

Figure 4. One-dimensional streamwise and spanwise energy spectra. $Re_\tau = 180$.

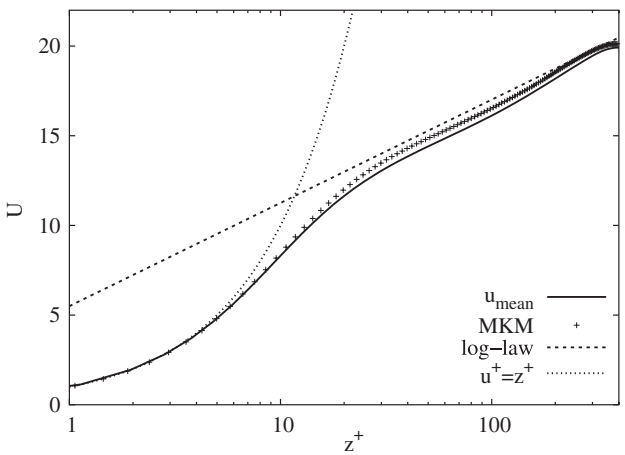

Figure 5. Mean velocity profile. $Re_\tau = 395$.

4. *A PRIORI* TESTS OF LES

In this section, we discuss the *a priori* tests of the explicit filtering. First, we discuss the tests where two-dimensional filtering was applied. In Section 4.1, the traditional approach, where the whole velocity field is filtered, is applied, and in Section 4.2, only the non-linear convection term of the Navier–Stokes equations is filtered explicitly. In Section 4.3, we discuss the differences between the two approaches, and finally in Section 4.4, three-dimensional filtering is discussed.

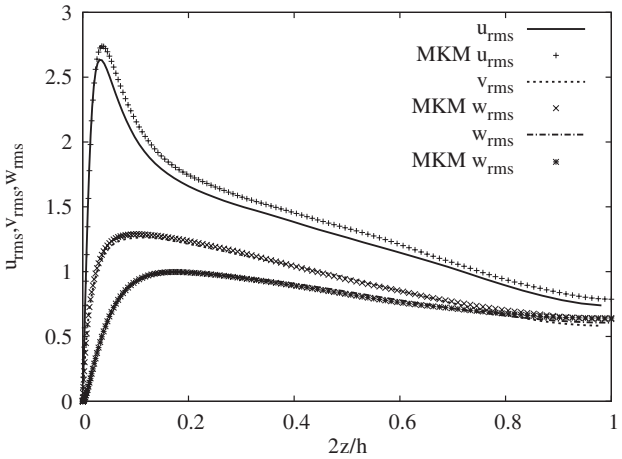

Figure 6. The RMS-velocity components. $Re_\tau = 395$.

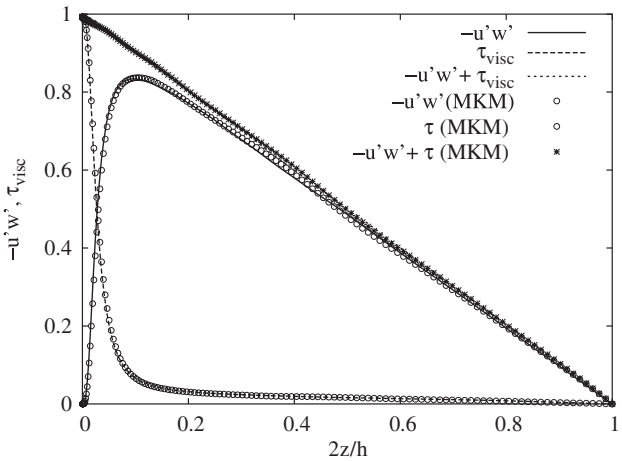

Figure 7. Total, viscous and turbulent stresses. $Re_\tau = 395$.

4.1. *Explicit filtering of the whole velocity field*

In the *a priori* tests we follow the approach suggested in Reference [4]. The filtered Navier–Stokes equations, that are being solved in LES in the incompressible case, are written as

$$\frac{\partial \bar{\tilde{u}}_i}{\partial t} + \frac{\partial \bar{\tilde{u}}_i \bar{\tilde{u}}_j}{\partial x_j} = -\frac{\partial \bar{\tilde{p}}}{\partial x_i} + \frac{\partial}{\partial x_j}\left(\frac{1}{Re_\tau}\left(\frac{\partial \bar{\tilde{u}}_i}{\partial x_j} + \frac{\partial \bar{\tilde{u}}_j}{\partial x_i}\right)\right) - \alpha_i \tag{7}$$

where tilde refers to the implicit grid filter, overline to the explicit filter and α_i is the SGS term that requires modelling. The relation between the exact non-linear term and its discrete

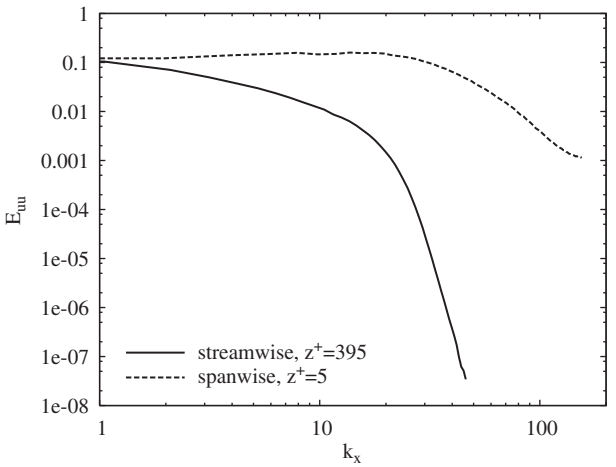

Figure 8. One-dimensional streamwise and spanwise energy spectra. $Re_\tau = 395$.

counterpart may be written as

$$\frac{\partial \widetilde{\overline{u_i}\overline{u_j}}}{\partial x_j} = \frac{\Delta \bar{\tilde{u}}_i \bar{\tilde{u}}_j}{\Delta x_j} + \underbrace{\frac{\partial \widetilde{\overline{u_i}\overline{u_j}}}{\partial x_j} - \frac{\partial \bar{\tilde{u}}_i \bar{\tilde{u}}_j}{\partial x_j}}_{=\alpha_i} + \underbrace{\frac{\partial \bar{\tilde{u}}_i \bar{\tilde{u}}_j}{\partial x_j} - \frac{\Delta \bar{\tilde{u}}_i \bar{\tilde{u}}_j}{\Delta x_j}}_{=\beta_i} \tag{8}$$

where the product $\bar{\tilde{u}}_i \bar{\tilde{u}}_j$ can be evaluated from the resolved flow field, $\Delta/\Delta x_j$ is the difference approximation to the first derivative, α_i is the SGS term that needs modelling. It corresponds to the divergence of the SGS stress. β_i represents the numerical error related to the spatial discretization of the non-linear convection term. The viscous dissipation term is divided by the Reynolds number and it is thus small in comparison to convection, and the numerical error related to time integration is assumed to be small due to the small time step applied in the explicit time-integration method. This choice to study only the numerical error related to the convection term has also been made in previous *a priori* studies by other authors [4, 5].

The exact SGS term and the numerical error can be estimated from DNS data using Equation (8). One assumes that the DNS velocity field u_i is a good approximation to the exact solution. The DNS field is filtered using a filter with the width, Δ_f, equal to the LES grid spacing, Δ_{LES}, to obtain the field $\tilde{u}_i$ corresponding to the LES velocity field. In this study, a fourth-order commutative filter with the width of three grid spacings from Reference [11] was applied as the grid filter. If explicit filtering is studied, $\tilde{u}_i$ is filtered again applying a wider filter to obtain the explicitly filtered field $\bar{\tilde{u}}_i$. In this study, the trapezoidal filter was applied as the explicit filter. If the filter width of the trapezoidal filter is based on the standard deviation, it is slightly wider than the region over which the quantity being filtered in integrated [10]. However, if the width is based on the effective filter cut-off frequency as with the commutative filters [11], it is the same as the integration interval.

Both terms appearing in the definition of the SGS term, α_i, and the first term in the definition of the numerical error, β_i, are evaluated on the DNS grid, and the fourth-order central-difference scheme was applied. The fourth-order scheme was used to make the numerical

Table IV. Dimensions of the channel and resolution of the studied LES grid in the *a priori* tests at $Re_\tau = 180$.

	Streamwise	Spanwise	Wall-normal	
Length/channel half-height	8.0	4.0	2.0	2.0
Number of grid points	40	50	100	32
Resolution in wall units	36	14	6 (max)	14 (max)

Table V. Dimensions of the channel and resolution of the studied LES grid in the *a priori* tests at $Re_\tau = 395$.

	Streamwise	Spanwise	Wall-normal
Length/channel half-height	6.0	3.2	2.0
Number of grid points	53	53	120
Resolution in wall units	45	24	15 (max)

error related to these terms as small as possible. Since the DNS result was obtained using a second-order scheme, the accuracy of the prediction of these terms is however not of fourth order.

The second term in the definition of the numerical error β_i is evaluated on the LES grid. The grid filtered velocity field $\tilde{u}_i$ is restricted to the LES grid, it is filtered explicitly on the LES grid, products $\bar{\tilde{u}}_i\bar{\tilde{u}}_i$ are evaluated on the cell boundaries using a second-order interpolation and finally the second-order central-difference scheme is applied on this coarser grid. The points of the LES grid match the DNS grid, and thus, no interpolation is applied when the filtered field is restricted to the DNS grid. Explicit filtering is here performed on the LES grid because this term represents the derivative evaluated in LES, and in actual LES the velocity field is filtered on the LES grid. This differs somewhat from the choice made by other authors [4, 5], but this was considered more consistent. However, when the different approaches were tested, this had no effect on the conclusions.

The resolutions of the studied LES grids at the two Reynolds numbers are given in Tables IV and V. The grid spacing of the studied LES grid in the streamwise and spanwise direction, Δ_{LES}, was three times the grid spacing of the corresponding DNS grid. Actual channel flow simulations applying similar resolutions have been performed by other authors [5, 8, 17]. In the first set of the *a priori* tests, both filters were applied only in the homogeneous directions, and the LES grid had the same resolution in the wall-normal direction as the original DNS grid had. This approach has been applied in the previous *a priori* tests of the channel flow [5, 18].

Only the SGS term and the numerical error of the streamwise momentum equation were studied. The spanwise and wall-normal momentum equations have been studied by other authors, and the behaviour was similar to the streamwise equation [5].

In Figure 9, we see how the L_2-norms of the numerical error, β_x, and of the exact SGS term, α_x, behaved in the *a priori* tests at $Re_\tau = 180$. The L_2-norms were first evaluated over the homogeneous directions. To insure that the results are not due to statistical variation, the norms were evaluated also over 30 non-dimensional time units. However, because of the averaging over the homogeneous directions, including the time averaging only made the curves

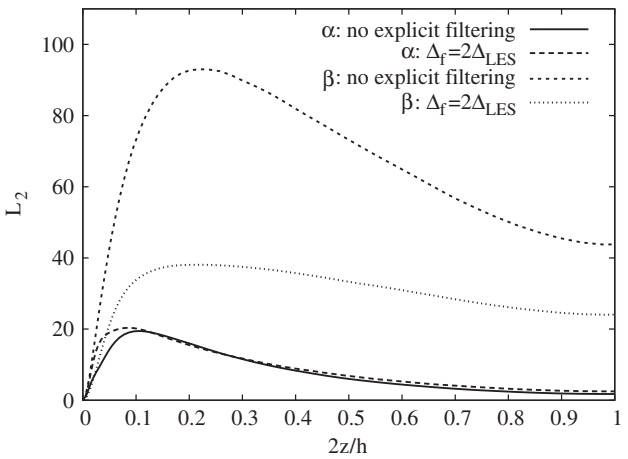

Figure 9. L_2-norms of the SGS term, α, and numerical error, β. The whole velocity field is filtered. $Re_\tau = 180$.

smoother, and it did not affect the conclusions. When explicit filtering was not applied, the L_2-norms $\|\beta_x\|_2$ and $\|\alpha_x\|_2$ were of the same magnitude only in the near-wall region. For the most part, $\|\beta_x\|_2$ was much larger than $\|\alpha_x\|_2$. As the explicit filter of the width of two LES grid spacings ($\Delta_f = 2\Delta_{LES}$) was applied, the magnitude of the numerical error diminished. However, the SGS term α_x did not grow as fast as the numerical error β_x diminished, and the numerical error still dominated the SGS term in most part of the channel. The same type of behaviour has also been noticed in the previous studies [5].

In principle, increasing the filter width further would lead to a situation where $\|\beta_x\|_2$ is smaller than $\|\alpha_x\|_2$. However, on a fixed grid resolution, this situation would not be physically meaningful and in addition, it would be computationally inefficient. In Figure 10, we see the behaviour of $\|\alpha_x\|_2$ from the cases where larger filter widths were applied. We notice that when the filter width was large enough, the growth of the SGS term stopped and it actually began to diminish. First, only in a small area, but later in the whole channel. This behaviour is in contradiction with the idea of explicit filtering. However, it is understood by studying the energy spectra and the cut-off wave number. The minimum wavelength that the grid was able to describe is two times the grid spacing, Δ. Thus, the maximum wave number scaled by the channel half-height, δ, is

$$\hat{k}_{\max}\delta = \frac{2\pi}{2\Delta/\delta} \tag{9}$$

In the current DNS, the maximum wave numbers in the streamwise and spanwise directions were $\hat{k}^x_{\max}\delta \approx 47$ and $\hat{k}^y_{\max}\delta \approx 118$, respectively. On the studied LES grid with no explicit filtering, these wave numbers were 12 and 30, respectively. When the spectra in Figure 4, are considered, these cut-off wave numbers seem to be reasonable. When explicit filtering is applied, the effective resolution is determined by the filter width Δ_f. Thus, also the cut-off wave number is determined by Δ_f. When the explicit filter of the width of $\Delta_f = 4\Delta_{LES} = 12\Delta_{DNS}$ was applied, the cut-off wave number in the streamwise direction was approximately

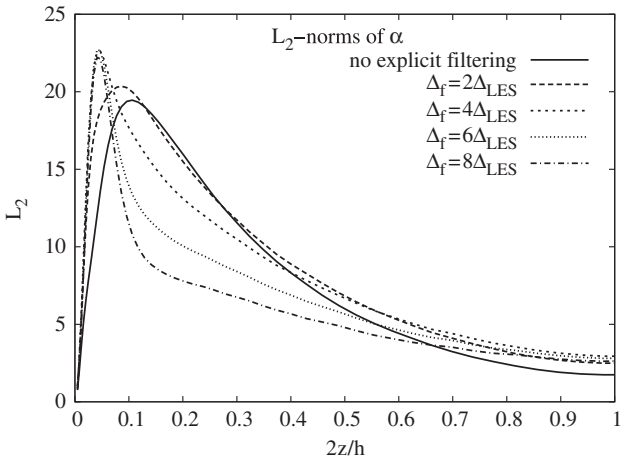

Figure 10. L_2-norm of the SGS term using also wider filters. The whole velocity field is filtered. $Re_\tau = 180$.

$\hat{k}^x_{\max}\delta \approx 3$ and in the spanwise direction $\hat{k}^y_{\max}\delta \approx 10$. The energy spectra from the area where the undesired behaviour of the SGS term began ($y/h \approx 0.05$, $y^+ \approx 36$) are also included in Figure 4. We notice that as the explicit filter is applied, both the streamwise and spanwise cut-off wave numbers are quite low. As the filter width is increased further, the cut-off wave numbers become even smaller. Thus, one reason for the unphysical behaviour of the SGS term is that the filter width had become too large and also the large energy-bearing scales were affected by the filter. Thus, the assumptions made in the derivation of the LES equations were contradicted.

When the SGS term is considered, there are two alternatives for the interpretation of the results. First, the obtained SGS term can be seen as the SGS term of a simulation on a reasonable LES grid applying explicit filtering. The other possibility is to interpret it as the SGS term of an LES performed on a grid with spacing equal to the filter width Δ_f and with no explicit filtering. Similar interpretation cannot be done for the numerical error. The resolution at which the magnitude of the SGS term started to diminish also gives a limit for the minimum resolution necessary in LES simulation of the channel flow at this Reynolds number. At a lower resolution, the grid-filtered momentum equations would no longer be meaningful. At this Reynolds number ($Re_\tau = 180$), the behaviour started when the grid spacing was eight times our DNS grid spacing. Thus, the LES grid would have the nominal resolution of $\Delta x^+ = 144$ and $\Delta y^+ = 56$. This would be quite a coarse LES grid.

In Figure 11, we see the behaviour of the L_2-norms of the SGS term and of the numerical error from the *a priori* tests performed at $Re_\tau = 395$. Here, the results were averaged over the homogeneous directions and 20 non-dimensional time units. As expected, in this case the magnitude of the SGS term was larger in the near-wall region than at the lower Reynolds number. However, the numerical error still dominated the SGS term. Explicit filtering diminished the numerical error, and in the near-wall region, $\|\alpha_x\|_2$ and $\|\beta_x\|_2$ were about the same size. However, our LES grid was quite coarse for explicit filtering, and thus, the SGS term did not grow with the filter width. In Figure 12, we have the L_2-norms of the SGS term from

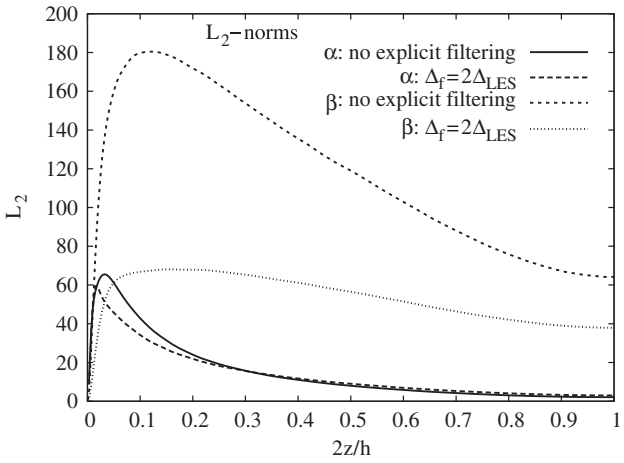

Figure 11. L_2-norms of the SGS term, α, and numerical error, β. The whole velocity field is filtered. $Re_\tau = 395$.

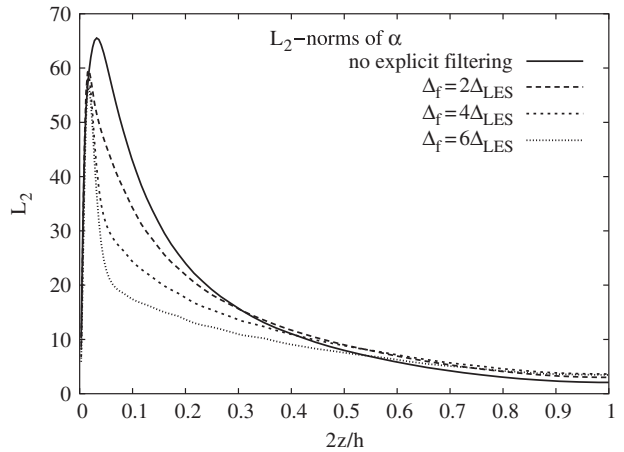

Figure 12. L_2-norm of the SGS term using also wider filters. The whole velocity field is filtered. $Re_\tau = 395$.

tests where also a wider filter was applied. In this case, the L_2-norm of the SGS term started to diminish already when the filter width was $\Delta_f = 2\Delta_{LES} = 6\Delta_{DNS}$. Thus, the LES results on this grid could not be improved using explicit filtering because the nominal resolution becomes too low.

Based on the results of this section, it seems that if one applies explicit filtering to the whole velocity field, one has to increase the grid resolution. Otherwise, the nominal resolution becomes too low and the SGS starts to behave in an unphysical manner. However, in LES, the computational capacity usually sets limits for the grid resolution. Thus, it seems that on a reasonable LES grid, explicit filtering of the whole velocity field is not a reasonable approach to reducing the numerical errors.

4.2. Explicit filtering of only the non-linear term

Next, we consider the approach to explicit filtering where the explicit filter is applied only to the non-linear convection term. This approach was suggested in Reference [10]. The equations being solved are written as

$$\frac{\partial \tilde{u}_i}{\partial t} + \frac{\partial \overline{\tilde{u}_i \tilde{u}_j}}{\partial x_j} = -\frac{\partial \tilde{p}}{\partial x_i} + \frac{\partial}{\partial x_j}\left(\frac{1}{Re_\tau}\left(\frac{\partial \tilde{u}_i}{\partial x_j} + \frac{\partial \tilde{u}_j}{\partial x_i}\right)\right) - \alpha_i \tag{10}$$

where the overline again refers to the explicit filter and the tilde to the implicit filter. The difference to Equation (7) is that the explicit filter is applied only to the non-linear convection term, and the other terms are affected only by the implicit filter. The SGS term α_i in Equation (10) is defined as

$$\alpha_i = \frac{\partial \widetilde{u_i u_j}}{\partial x_j} - \frac{\partial \overline{\tilde{u}_i \tilde{u}_j}}{\partial x_j} \tag{11}$$

and the numerical error β_i related to the spatial discretization of the SGS term as

$$\beta_i = \frac{\partial \overline{\tilde{u}_i \tilde{u}_j}}{\partial x_j} - \frac{\Delta \overline{\tilde{u}_i \tilde{u}_j}}{\Delta x_j} \tag{12}$$

Both definitions differ from Equation (8). We will see that the differences in the definition of the SGS term α_i are crucial. For discussion on how this modified α_i can be modelled in actual LES see e.g. Reference [9].

Explicit filtering of only the non-linear term was tested using the same methods as discussed in the previous section. The essential difference was that the explicit filter was applied only to the product of velocity components and not to the individual velocity components.

In Figures 13 and 14, we depict the L_2-norms of α_x and β_x from the case at $Re_\tau = 180$ and in Figures 15 and 16 from $Re_\tau = 395$ case. We notice that this filtering approach had indeed the desired effect on both numerical error and SGS term. The numerical error rapidly diminished and, in addition, the magnitude of the SGS term grew fast with the filter width. The SGS term was everywhere clearly larger than the numerical error. The undesired diminishing of the SGS term as the filter width grows was not noticed in this approach.

4.3. Difference between the two approaches

In this section, we further discuss some of the differences between the two applied approaches to explicit filtering. Firstly, we discuss the sum of the numerical error and the SGS term and secondly, the two definitions of the SGS term.

The sum of the SGS term and the numerical error can be interpreted as the difference between a sufficiently resolved and coarse-grid DNS solutions, i.e. an LES without an SGS model. For the case, where the whole velocity field is filtered, the sum is written as

$$\alpha_i + \beta_i = \frac{\partial \widetilde{u_i u_j}}{\partial x_j} - \frac{\partial \overline{\tilde{u}_i}\,\overline{\tilde{u}_j}}{\partial x_j} + \frac{\partial \overline{\tilde{u}_i}\,\overline{\tilde{u}_j}}{\partial x_j} - \frac{\Delta \overline{\tilde{u}_i}\,\overline{\tilde{u}_j}}{\Delta x_j} = \frac{\partial \widetilde{u_i u_j}}{\partial x_j} - \frac{\Delta \overline{\tilde{u}_i}\,\overline{\tilde{u}_j}}{\Delta x_j} \tag{13}$$

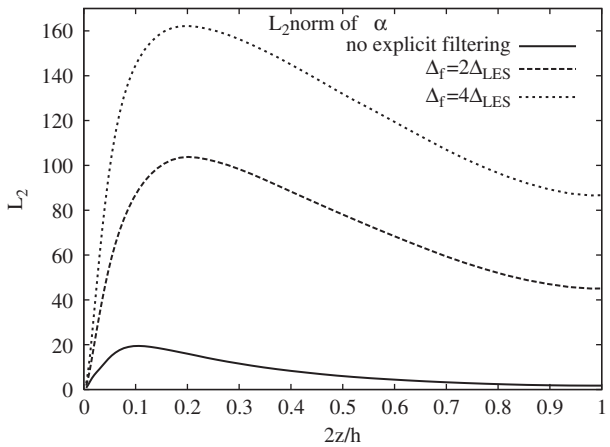

Figure 13. L_2-norm of the SGS term, α, using explicit filters of widths 2 and 4 LES grid spacings. Only the non-linear term is filtered. $Re_\tau = 180$.

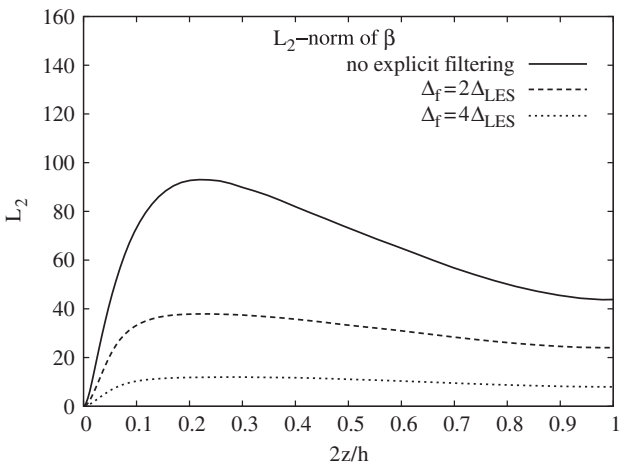

Figure 14. L_2-norm of numerical error, β, using explicit filters of widths 2 and 4 LES grid spacings. Only the non-linear term is filtered. $Re_\tau = 180$.

If only the non-linear term is filtered explicitly, the sum of α_i and β_i is written as

$$\alpha_i + \beta_i = \frac{\partial \widetilde{u_i u_j}}{\partial x_j} - \frac{\partial \overline{\tilde{u}_i \tilde{u}_j}}{\partial x_j} + \frac{\partial \overline{\tilde{u}_i \tilde{u}_j}}{\partial x_j} - \frac{\Delta \overline{\tilde{u}_i \tilde{u}_j}}{\Delta x_j} = \frac{\partial \widetilde{u_i u_j}}{\partial x_j} - \frac{\Delta \overline{\tilde{u}_i \tilde{u}_j}}{\Delta x_j} \tag{14}$$

This sum for both approaches at Reynolds number $Re_\tau = 180$ is plotted in Figures 17 and 18. We notice that in the first approach, the difference between the sufficiently resolved and the coarse-gird DNS diminished when explicit filtering was applied. This suggests, somehow misleadingly, that the results of a coarse-grid DNS could be improved simply by applying

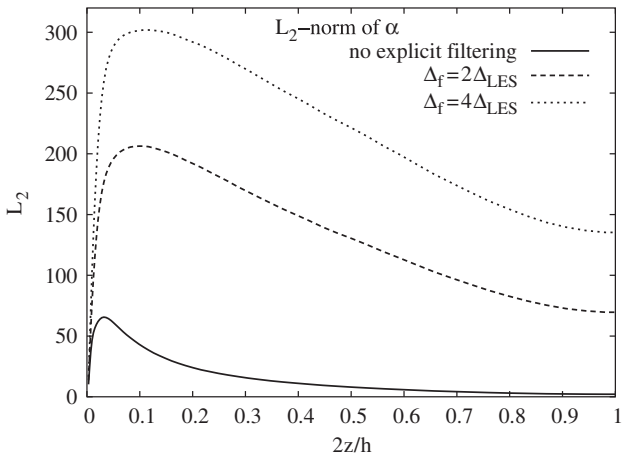

Figure 15. L_2-norm of the SGS term, α, using explicit filters of widths 2 and 4 LES grid spacings. Only the non-linear term is filtered. $Re_\tau = 395$.

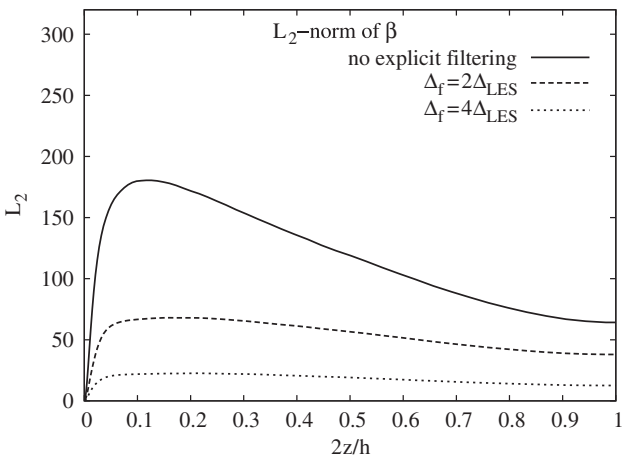

Figure 16. L_2-norms of numerical error, β, using explicit filters of widths 2 and 4 LES grid spacings. Only the non-linear term is filtered. $Re_\tau = 395$.

an explicit filter to the whole velocity field. In this case, the numerical error was effectively diminished, which led to the decreased difference between the sufficiently resolved and the coarse-grid DNS. Applying an SGS model could not improve these coarse-grid results, since the effect of the SGS term also diminished. Figure 17 thus demonstrates the fact that when the whole velocity field is filtered, some information is lost, and we cannot recover it by modelling. Figure 18 is from the case where only the non-linear term was filtered. In this case, the behaviour of the difference was the opposite. Increasing the filter width increased the

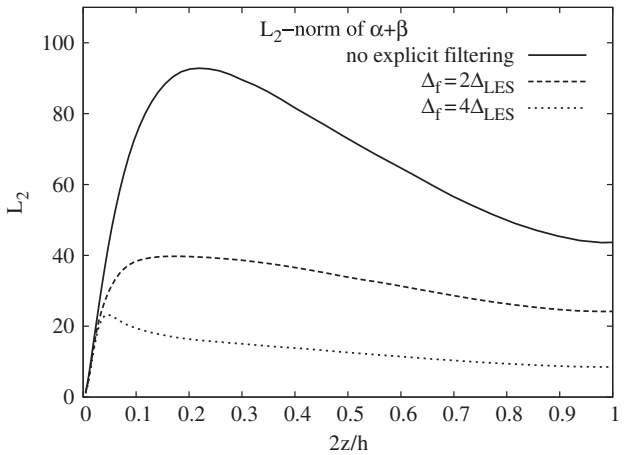

Figure 17. L_2-norm of the sum of the SGS term, α, and numerical error, β. The whole velocity field is filtered. $Re_\tau = 180$.

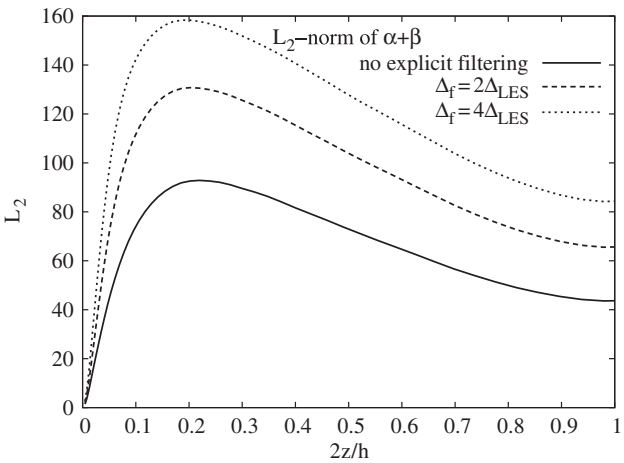

Figure 18. L_2-norm of the sum of the SGS term, α, and numerical error, β. Only the non-linear term is filtered. $Re_\tau = 180$.

difference between the sufficiently resolved and the coarse-grid DNS results. This indicates that at the same time as the numerical error decreased, the scales filtered out have been shifted to the SGS term, and using an SGS model could improve the results. This supports the conclusion that the latter method may lead to improved LES results.

Depending on whether the explicit filter was applied to the whole velocity field or only to the non-linear term, the behaviour of the SGS term α_i was clearly different. We next consider more carefully the origin of this difference. We label the SGS term of the first approach where

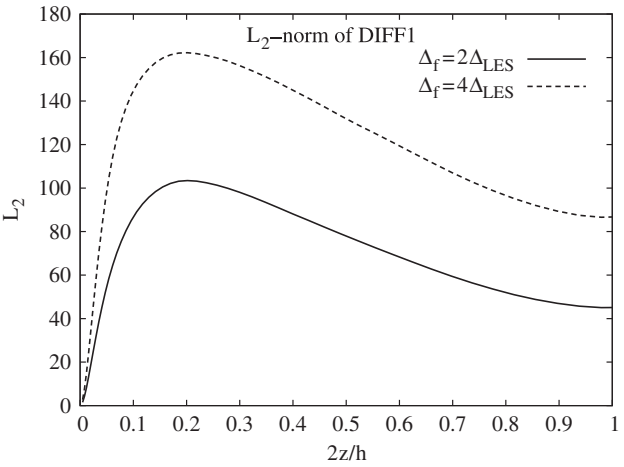

Figure 19. The difference between the definitions α^1 and α^2 for the SGS term. The difference in the resolved non-linear term. $Re_\tau = 180$.

the whole velocity field is filtered explicitly with the superscript 1

$$\alpha_i^1 = \frac{\partial \widetilde{\overline{u_i}\,\overline{u_j}}}{\partial x_j} - \frac{\partial \overline{\tilde{u}_i}\,\overline{\tilde{u}_j}}{\partial x_j} \tag{15}$$

and the SGS term of the second approach where explicit filtering is applied only to the non-linear term with the superscript 2

$$\alpha_i^2 = \frac{\partial \widetilde{u_i u_j}}{\partial x_j} - \frac{\partial \overline{\tilde{u}_i \tilde{u}_j}}{\partial x_j} \tag{16}$$

In both definitions for the SGS term α_i, tilde refers to the grid filter and overline to the explicit filter. The first term of α_i represents the non-linear term that appears in the filtered Navier–Stokes equations. The second term represents the quantity that is evaluated using only the resolved field. There are differences between the two definitions in both of these terms, and α_i^2 and α_i^1 are related to each other via the equation

$$\alpha_i^2 = \alpha_i^1 + \underbrace{\frac{\partial \widetilde{u_i u_j}}{\partial x_j} - \frac{\partial \widetilde{\overline{u_i}\,\overline{u_j}}}{\partial x_j}}_{=\text{DIFF1}} + \underbrace{\frac{\partial \widetilde{\overline{u_i}\,\overline{u_j}}}{\partial x_j} - \frac{\partial \overline{\tilde{u}_i \tilde{u}_j}}{\partial x_j}}_{=\text{DIFF2}} \tag{17}$$

The difference between α_i^1 and α_i^2 consists of two parts: the difference in the resolved non-linear term in the filtered Navier–Stokes equations (DIFF1) and the quantity being evaluated from the resolved field (DIFF2). DIFF1 represents the sub-filter part of $\partial \widetilde{u_i u_j}/\partial x_j$, and DIFF2 is the divergence of the sub-filter-scale stress or Leonard stress. The L_2-norms of these two terms are depicted in Figures 19 and 20 with varying explicit filter widths. Both of these terms increased with increasing filter width, but the difference in the resolved non-linear term (DIFF1) formed the major part of the difference between the two definitions of α_i. It seems

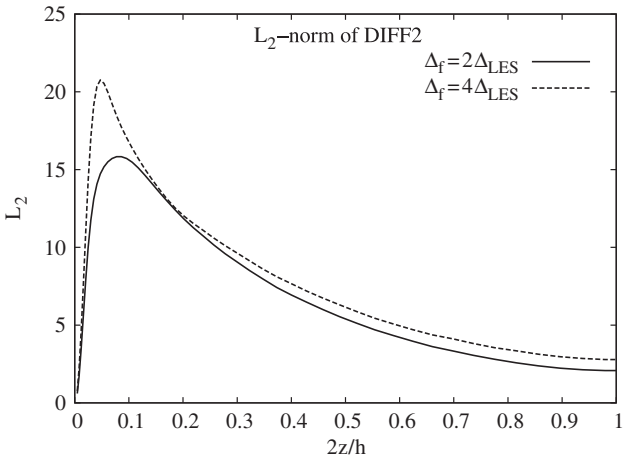

Figure 20. The difference between the definitions α^1 and α^2 for the SGS term. The difference in the term evaluated from the resolved field. $Re_\tau = 180$.

that, in the behaviour of the SGS term, the crucial point is the interpretation of the non-linear term of the filtered Navier–Stokes equations.

4.4. Three-dimensional filtering

In the *a priori* tests discussed in the previous sections, filtering was applied only in the homogeneous directions, and the wall-normal resolution of the LES grid was the same as the resolution of the DNS grid. In this section, we discuss *a priori* tests in which filtering was applied also in the wall-normal direction, and the resolution in this direction corresponded to a resolution of a normal LES grid (see Table IV). Both filtering of the whole velocity field and filtering of the non-linear term only are studied here at the Reynolds number $Re_\tau = 180$. Filtering in inhomogeneous directions is an important issue, since in real applications of LES, homogeneous directions are rather an exception. The aim of these tests is to verify that the results of the previous sections are not restricted to cases with only homogeneous directions.

Applying filtering in the wall-normal direction is not as straightforward as in the homogeneous directions, because the grid spacing varies and changing the order of the derivative and the filter introduces commutation errors. Commutative filters have been proposed [11] and applied in actual simulations [8], and they can also be applied in the *a priori* tests. The same symmetrical fourth-order commutative filter as applied in the homogeneous directions was used in the wall-normal direction in the middle of the domain. In the near-wall region, asymmetrical commutative filters were constructed following the method presented in Reference [11]. Since these filters are applied as grid filters, they should have the effective filter width of three DNS grid spacings. In addition, they should have as low commutation error as possible, since the commutation error adds to the error in evaluation of the SGS term α_i and of the numerical error β_i on the DNS grid. However, in order to avoid large negative

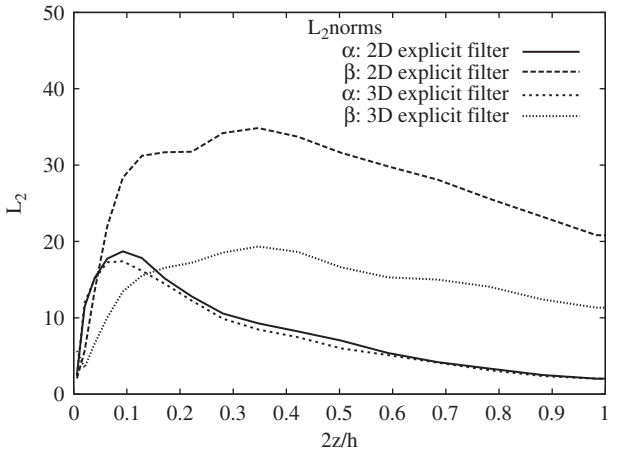

Figure 21. Numerical error and SGS term using three-dimensional grid filter and two- and three-dimensional explicit filters. The whole velocity field is filtered explicitly. $\Delta_f = 2\Delta_{LES}$. '2D': three-dimensional grid filter and two-dimensional explicit filtering. '3D': both filters were three dimensional. $Re_\tau = 180$.

and positive values of the filter function in the near-wall region, the order of the filter was reduced in the three points of the DNS grid that were closest to the walls.

The last term of the numerical error β_i (Equation (12)) is evaluated on the LES grid, and also the explicit filtering is performed there. The trapezoidal filter has the commutation error of second order, and since the second-order central-difference scheme is applied on the LES grid, it is a suitable choice also for the three-dimensional filtering.

Three of the terms of α and β are evaluated on the DNS grid (Equations (8), (11) and (12)). Thus, the velocity field is filtered, but it is not restricted to the LES grid, and also the explicit filter has to be applied on the DNS grid. The explicit filter applied on the DNS grid has to have filter width of six DNS grid spacings. The derivatives on the DNS grid were evaluated using the fourth-order central-difference scheme and the grid filter was of fourth order. Thus, we would like to have also a fourth-order explicit filter. This makes the construction of the explicit filter somewhat problematic on the DNS grid. To obtain a filter transfer function that has that long filter width and behaves well, i.e. does not have large negative or positive values, one has to fix at least four derivatives of the filter transfer function at the grid cut-off frequency. This is why a filter that is only of second order was applied as the explicit filter on the DNS grid. This introduces a commutation error of order Δ_{DNS}^2 to the corresponding terms of α_i and β_i. However, the error on the LES grid is of the order Δ_{LES}^2, and the numerical error on the DNS grid is still too small to affect the conclusions of the *a priori* tests.

The results from the *a priori* tests applying three-dimensional filtering to the whole velocity field are given in Figure 21. Here the L^2-norms were evaluated on a single time step. In the case with label '2D', only the grid filter was three dimensional and the explicit filter was two dimensional, and finally in case '3D', both grid and explicit filters were three dimensional. Applying the three-dimensional explicit filter reduced further the numerical error. This is natural, since the LES velocity field becomes somewhat smoother due to the filtering performed

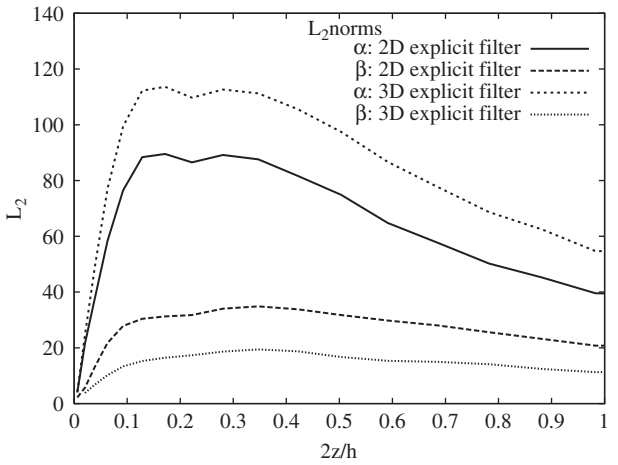

Figure 22. Numerical error and SGS term. Only the non-linear term is filtered explicitly. $\Delta_f = 2\Delta_{LES}$. '2D': three-dimensional grid filter and two-dimensional explicit filtering. '3D': both filters were three dimensional. $Re_\tau = 180$.

in the wall-normal direction. When the three-dimensional explicit filter was applied, the SGS term diminished slightly. This is again undesired behaviour, and it is due to the damping of the large-scale eddies.

The numerical error and the SGS term from the tests where only the non-linear term was filtered are depicted in Figure 22. We notice the same behaviour of the numerical error as in the previous case, while here the SGS term grew when the three-dimensional explicit filter was applied. In addition, the SGS term was everywhere much larger than the numerical error. Thus, also explicit three-dimensional filtering of only the non-linear term led to the desired result.

The results presented in this section thus verify that applying filtering only in homogeneous directions in *a priori* tests did not affect the overall conclusion of the Sections 4.1–4.3. When three-dimensional filtering was applied, filtering of the whole velocity field seemed to lead to an unphysical situation. The desired behaviour of filtering only the non-linear term was further reinforced when the three-dimensional filter was applied.

5. CONCLUSIONS

This paper concentrated on the role of numerical error in large eddy simulation. The aim was to clarify how well explicit filtering is suited to reducing numerical errors in a practical LES, where low-order finite-difference schemes are applied, and as the explicit filter is applied, the grid resolution is not increased.

Two approaches to explicit filtering were discussed and compared *a priori*: filtering of the whole velocity field and filtering of the non-linear convection term of the Navier–Stokes equations. When the whole velocity field was filtered while the grid resolution was kept

constant, filtering did not increase the SGS term, and finally when the filter width was increased further, the SGS term started to diminish. One reason for this unphysical behaviour is that the large energy-bearing eddies were affected by the filter. This began already when a filter width of four grid spacings was applied. This filter width combined with the second-order central-difference scheme has been previously suggested by some groups [2, 4]. Based on the results presented in this paper, it seems that to increase the effect of the SGS model using this approach one would have to increase also the grid resolution. Usually, this is not possible because of the increased computational demands.

When only the non-linear term was filtered, the desired behaviour was obtained. As the filter width was increased, the L_2-norm of the numerical error diminished and that of the SGS term increased. The numerical error was clearly smaller than the SGS term. The increased SGS term indicates that in an actual simulation, the role of the chosen SGS model is pronounced, and the responsibility for scales being filtered out is shifted to the model. Thus, an SGS model can improve the simulation results. By studying the sum of the numerical error and the SGS term, it was further demonstrated that while filtering of the whole velocity field leads to loss of information, sub-filter-scale motions are effectively shifted to the SGS term if the non-linear convection term in filtered.

The main difference between the two discussed approaches to explicit filtering is the interpretation of the resolved non-linear term in the filtered Navier–Stokes equations. In the first approach, where the whole velocity field is filtered, one tries to model the non-linear term that has been explicitly filtered. In the second approach, where the explicit filter has been applied only to the non-linear terms, one tries to model the grid-filtered term.

In the previous *a priori* studies of the channel flow, filtering has been applied only in the homogeneous directions. However, in many applications, there are no homogeneous directions. In this paper, *a priori* tests applying filtering in the wall-normal direction were presented. We noticed that including this filtering reinforced the overall conclusion. The unphysical behaviour of the SGS term in the case, where the whole velocity field was filtered explicitly, remained. The desired behaviour when only the non-linear term was filtered was even stronger with the three-dimensional filtering. Thus, the conclusions from the tests with filtering in homogeneous directions can be extended to cases with inhomogeneous directions. This suggests that explicit filtering is an effective method for reducing numerical errors also in practical applications with inhomogeneous directions. In cases where there are homogeneous directions, there is also the possibility to apply the filtering only in these directions. Based on the present results, it seems that filtering also in inhomogeneous directions further increases the difference between the numerical error and the SGS term. On the other hand, filtering in inhomogeneous directions further increases the computational cost, while improved results can be obtained with filtering applied only in the homogeneous directions.

Based on these *a priori* tests, it seems that explicit filtering of the non-linear term could be an efficient way to control the level of numerical errors in LES. In this approach, the responsibility for the sub-filter scales is effectively shifted to the SGS model, and in simulations applying explicit filtering, advanced SGS models are probably required.

ACKNOWLEDGEMENTS

This work has been funded by the Finnish National Graduate School in Computational Fluid Dynamics and the Finnish Cultural Foundation. The computer capacity was provided by CSC, Scientific Computing

Ltd. The used channel-flow code is based on a code written by Dr Boersma from TU Delft. These contributions are gratefully acknowledged.

REFERENCES

1. Moin P, Mahesh K. Direct numerical simulation: a tool in turbulence research. *Annual Reviews of Fluid Mechanics* 1998; **30**:539–578.
2. Ghosal S. An analysis of numerical errors in large-eddy simulations of turbulence. *Journal of Computational Physics* 1996; **125**:187–206.
3. Kravchenko AG, Moin P. On the effect of numerical errors in large eddy simulations of turbulent flows. *Journal of Computational Physics* 1997; **131**:310–322.
4. Vreman B, Geurts B, Kuerten H. Discretization error dominance over subgrid terms in large eddy simulation of compressible shear layers in 2D. *Communications in Numerical Methods in Engineering* 1994; **10**:785–790.
5. Majander P, Siikonen T. Evaluation of Smagorinsky-based subgrid-scale models in a finite-volume computation. *International Journal for Numerical Methods in Fluids* 2002; **40**:735–774.
6. Chow FK, Moin P. A further study of numerical errors in large-eddy simulations. *Journal of Computational Physics* 2003; **184**:366–380.
7. Lund TS, Kaltenbach H-J. Experiments with explicit filtering for LES using a finite-difference method. *Center for Turbulence Research*, *Annual Research Briefs*, Stanford University, 1995; 91–105.
8. Gullbrand J. Explicit filtering and subgrid-scale models in turbulent channel flow. *Center for Turbulence Research*, *Annual Research Briefs*, Stanford University, 2001; 31–42.
9. Gullbrand J. Grid-independent large-eddy simulation in turbulent channel flow using three-dimensional explicit filtering. *Center for Turbulence Research*, *Annual Research Briefs*, Stanford University, 2002; 167–179.
10. Lund TS. On the use of discrete filters for large eddy simulation. *Center for Turbulence Research*, *Annual Research Briefs*, Stanford University, 1997; 83–95.
11. Vasilyev OV, Lund TS, Moin P. A general class of commutative filters for LES in complex geometries. *Journal of Computational Physics* 1998; **146**(1):82–104.
12. Harlow FH, Welch JE. Numerical calculation of time-dependent viscous incompressible flow of fluid with free surface. *Physics of Fluids* 1965; **8**(12):2182–2189.
13. Morinishi Y, Lund TS, Vasilyev OV, Moin P. Fully conservative higher order finite difference schemes for incompressible flow. *Journal of Computational Physics* 1998; **143**:90–124.
14. Lundbladh A, Berlin S, Skote M, Hildings C, Choi J, Kim J, Henningson D. An efficient spectral method for simulation of incompressible flow over a flat plate. *Technical Report 11*, Royal Institute of Technology, Department of Mechanics, Stockholm, Sweden, 1999.
15. Tennekes H, Lumley JL. *A First Course on Turbulence* (8th edn). MIT Press: Cambridge, MA, 1972.
16. Moser RD, Kim J, Mansour NN. Direct numerical simulation of turbulent channel flow up to $Re_\tau = 590$. *Physics of Fluids* 1999; **11**(4):943–945.
17. Piomelli U, Moin P, Ferziger JH. Model consistency in large eddy simulation of turbulent channel flow. *Physics of Fluids* 1988; **31**(7):1884–1891.
18. Brandt T. Discretization errors in LES using second-order central-difference scheme. In *European Congress on Computational Methods in Applied Sciences and Engineering*, Jyväskylä, Finland, July 2004, Neittaanmäki P, Rossi T, Majava K, Pironneau O (eds). ECCOMAS 2004.

